Frontiers of Physics
https://doi.org/10.1007/s11467-021-1105-6
Front. Phys.
17(2), 22502 (2022)

RESEARCH ARTICLE

Single-photon-level light storage with distributed Rydberg excitations in cold atoms

Hanxiao Zhang[1], Jinhui Wu[1,†], M. Artoni[2], G. C. La Rocca[3]

[1] *Center for Quantum Sciences and School of Physics, Northeast Normal University, Changchun 130024, China*
[2] *Department of Engineering and Information Technology and Istituto Nazionale di Ottica (INO-CNR), Brescia University, 25133 Brescia, Italy*
[3] *Scuola Normale Superiore and CNISM, 56126 Pisa, Italy*
Corresponding author. E-mail: †jhwu@nenu.edu.cn
Received May 12, 2021; accepted July 14, 2021

We present an improved version of the superatom (SA) model to examine the slow-light dynamics of a few-photons signal field in cold Rydberg atoms with van der Waals (vdW) interactions. A main feature of this version is that it promises consistent estimations on total Rydberg excitations based on dynamic equations of SAs or atoms. We consider two specific cases in which the incident signal field contains more photons with a smaller detuning or less photons with a larger detuning so as to realize the single-photon-level light storage. It is found that vdW interactions play a significant role even for the slow-light dynamics of a single-photon signal field as distributed Rydberg excitations are inevitable in the picture of dark-state polariton. Moreover, the stored (retrieved) signal field exhibits a clearly asymmetric (more symmetric) profile because its leading and trailing edges undergo different (identical) traveling journeys, and higher storage/retrieval efficiencies with well preserved profiles apply only to weaker and well detuned signal fields. These findings are crucial to understand the nontrivial interplay of single-photon-level light storage and distributed Rydberg excitations.

Keywords few-photons light storage, distributed Rydberg excitation, cold Rydberg atom, improved superatom model

1 Introduction

In the 20th century, people have been guided by extensive studies in optics and photonics into the intriguing world of quantum physics and quantum information. Photon-based schemes exhibiting obvious advantages like fast and parallel operations have flourished in both quantum communication and quantum computation tasks, including long-range secure quantum cryptography [1, 2], quantum repeater [3], and quantum information encoding [4]. It is still a great challenge, however, to achieve effective interactions between individual photons, though various schemes have been proposed to generate strongly interacting photons based, e.g., on cavity quantum electrodynamics systems assisted with atoms [5–7].

Interactions of photons may also be achieved through electromagnetically induced transparency (EIT), a well-known quantum interference effect that can largely modify near-resonant optical properties of coherently driven atomic media and metamaterials [8–10]. For instance, EIT can significantly enhance the Kerr nonlinearity and well suppress the linear absorption, both needed to achieve effective photonic phase gates [11–13]. Rydberg atoms, on the other hand, have been widely exploited to seek alternative quantum manipulation schemes, not only because they exhibit long radiative lifetimes and strong dipole-dipole interactions [14], but also because they are easy to combine with the EIT techniques [15–17]. Within this context, Rydberg-EIT media have been used to achieve single photon manipulation [18–21], cooperative optical nonlinearity [22], and photons bound states [23–25].

Neighboring Rydberg atoms exhibit, in turn, strong van der Waals (vdW) interactions that may lead to dipole blockade [26–29], known to prohibit the simultaneous excitations of two (or more) atoms to the same and different Rydberg states. A superatom (SA) model [30, 31] in the mean-field sense is commonly adopted to treat the nonlinear spectra based on dipole blockade in Rydberg-EIT media. This effective model has been extended [32] to partially recover experiments on slow-light propagation in cold Rydberg atoms [33–39], where intriguing effects such as sub-Poissonian statistics, storage enhanced interactions, and microwave induced exchanges of Rydberg dark-state polaritons are recently observed. On a differ-

* This article can also be found at http://journal.hep.com.cn/fop/EN/10.1007/s11467-021-1105-6.

ent tack and unrelated to the SA model, efforts have also been made [40–43] to devise theoretical schemes that deal with slow-light propagation and interaction in Rydberg-EIT media. These are schemes based, e.g., on open spin or effective field theories that use different degrees of approximation to relax the complexity of many-body photon(s) propagation problems in actual experiments.

In this paper we address the nontrivial interplay between spatially distributed Rydberg excitations and nonlinear light storage in a Rydberg-EIT medium, based on an improved SA model enabling deeper insights into the slow-light dynamics of a few-photons signal. This model provides consistent estimates on the total Rydberg excitations during light storage via two independent integration procedures, while ensuring an effective coupling to Rydberg atoms even if the signal is in the single-photon state. Our findings are supported by numerical calculations carried out for both an incident well detuned weaker signal and an incident nearly resonant stronger signal. We confirm, in particular, that vdW interactions ought to be taken into account even for a single-photon signal pulse as its slow-light dynamics must result in a dark-state polariton [43] with distributed Rydberg excitations. We also observe that the stored (retrieved) signal has a clearly asymmetric (more symmetric) profile as its leading and trailing edges suffer fairly different (roughly identical) nonlinear absorption and dispersion while propagating through the Rydberg-EIT medium. Last but not least, it is found that weaker and well detuned incident signals are largely insensitive to the nonlinear absorption and dispersion arising from distributed Rydberg excitations and hence are beneficial to improve the storage/retrieval efficiency and preserve the space-time profile.

2 Model and methods

Here we examine the storage and retrieval dynamics of a *quantum signal pulse* of electric field (frequency) $\hat{\mathcal{E}}_s$ (ω_s) traveling along the z axis in a cold sample of stationary atoms illuminated by a *classical control beam* of amplitude (frequency) E_c (ω_c) [see Fig. 1(a)]. Relevant Rabi frequencies and detunings are defined, respectively, as $\Omega_s = \kappa\mathcal{E}_s$, $\Omega_c = E_c d_{er}/(2\hbar)$ and $\delta = \omega_s - \omega_{ge}$, $\Delta = \omega_s + \omega_c - \omega_{gr}$ [see Fig. 1(b)]. Here d_{ij} (ω_{ij}) denotes the dipole moment (resonant frequency) on transition $|i\rangle \leftrightarrow |j\rangle$ while $\kappa = d_{ge}\sqrt{\omega_s/(2\hbar\varepsilon_0 V)}$ represents the coupling constant for signal photons of quantum volume V. The atoms exhibit a three-level ladder configuration involving the ground state $|g\rangle$, the intermediate state $|e\rangle$, and the Rydberg state $|r\rangle$, a pair of which located respectively at z and z' will interact through the vdW potential $\mathcal{V}(z-z') = C_6/|z-z'|^6$ when both excited to the Rydberg state. The vdW coefficient takes the value $C_6 = 6.5\times 2\pi\times 10^{12} s^{-1}\mu\text{m}^6$ in the case of $|g\rangle \equiv \left|5S_{1/2}, F=2, m_F=2\right\rangle$, $|e\rangle \equiv \left|5P_{3/2}, F=3, m_F=3\right\rangle$,

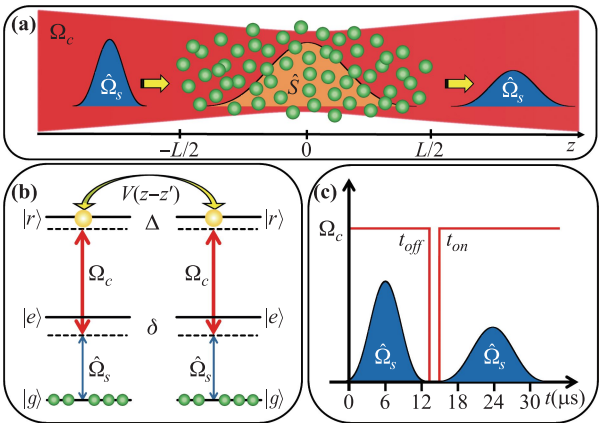

Fig. 1 **(a)** Schematic illustration of a storage and retrieval process where the *slow-light* signal field $\hat{\mathcal{E}}_s$ (Ω_s) is mapped into and then recovered from the *stationary* spin field $\hat{S}$ in a sample of cold atoms by switching off and then back on the control field E_c (Ω_c). **(b)** A ladder level configuration driven by the signal field of Rabi frequency (detuning) Ω_s (δ) on transition $|g\rangle \leftrightarrow |e\rangle$ and the control field of Rabi frequency (detuning) Ω_c ($\Delta-\delta$) on transition $|e\rangle \leftrightarrow |r\rangle$. Two atoms also exhibit the separation-dependent vdW potential $\mathcal{V}(z-z')$ when both are in Rydberg state $|r\rangle$. **(c)** A time sequence for the storage and retrieval process, in which field $\hat{\Omega}_s$ is incident at $t=0$ while field Ω_c is switched off (on) at t_{off} (t_{on}).

and $|r\rangle \equiv \left|83S_{1/2}, m_J = 1/2\right\rangle$ for the ^{87}Rb atoms [44]. A typical three-stage (time) excitation sequence for a signal taken in the form of a Gaussian pulse (see Section 3) is illustrated in Fig. 1(c). We further introduce the polarization $\hat{P} = \sqrt{N}\hat{\sigma}_{ge}$ and the spin field $\hat{S} = \sqrt{N}\hat{\sigma}_{gr}$ in terms of the atomic transition operators $\hat{\sigma}_{ge} = |g\rangle\langle e|$ and $\hat{\sigma}_{gr} = |g\rangle\langle r|$ [45], with N denoting the homogeneous atomic density. In the limit of low atomic excitations ($\sigma_{ge}\to 0$ and $\sigma_{gr}\to 0$) [46], these operators satisfy the same-time commutation relations $[\hat{\mathcal{E}}_s(z,t), \hat{\mathcal{E}}_s^\dagger(z',t)]/V = [\hat{P}(z,t), \hat{P}^\dagger(z',t)] = [\hat{S}(z,t), \hat{S}^\dagger(z',t)] = \delta(z-z')$.

Then we can write down the Hamiltonians [47]

$$
\begin{aligned}
\hat{H}_{tot} &= \hat{H}_{ph} + \hat{H}_{cp} + \hat{H}_{int},\\
\hat{H}_{ph} &= -\mathrm{i}\hbar c\int_0^L \mathrm{d}z\hat{\mathcal{E}}_s^\dagger(z,t)\partial_z\hat{\mathcal{E}}_s(z,t),\\
\hat{H}_{cp} &= -\hbar\int_0^L \mathrm{d}z[\sqrt{N}\hat{\Omega}_s^\dagger(z,t)\hat{P}(z,t) + h.c.]\\
&\quad -\hbar\int_0^L \mathrm{d}z[\Omega_c(t)\hat{S}^\dagger(z,t)\hat{P}(z,t) + h.c.]\\
&\quad -\hbar\int_0^L \mathrm{d}z[\delta\hat{P}^\dagger(z,t)\hat{P}(z,t) + \Delta\hat{S}^\dagger(z,t)\hat{S}(z,t)],\\
\hat{H}_{int} &= \frac{\hbar}{2}\int_0^L\int_0^L \mathrm{d}z\mathrm{d}z'[\hat{S}^\dagger(z,t)\hat{S}^\dagger(z',t)\\
&\quad \mathcal{V}(z-z')\hat{S}(z',t)\hat{S}(z,t)],
\end{aligned}
\tag{1}
$$

where the contributions $\hat{H}_{ph}$, $\hat{H}_{cp}$, and $\hat{H}_{int}$ have the usual interpretations [47] with respect to the kinetic energy,

atom-photon couplings, and dipole-dipole interactions, respectively. The corresponding Heisenberg equations can be obtained from $\hat{H}_{tot}$ and read as

$$\begin{aligned}
\partial_t\hat{P} &= -(\gamma_e - \mathrm{i}\delta)\hat{P} + \mathrm{i}\Omega_c^*\hat{S} + \mathrm{i}\sqrt{N}\hat{\Omega}_s,\\
\partial_t\hat{S} &= -[\gamma_r - \mathrm{i}(\Delta - \Delta_v)]\hat{S} + \mathrm{i}\Omega_c\hat{P},\\
\partial_t\hat{\Omega}_s &= -c\partial_z\hat{\Omega}_s + \mathrm{i}\kappa^2 V\sqrt{N}\hat{P},
\end{aligned} \tag{2}$$

where γ_e (γ_r) is the dephasing rate on transition $|g\rangle \leftrightarrow |e\rangle$ ($|e\rangle \leftrightarrow |r\rangle$). It is worth noting that the nonlocal term Δ_v denotes the expectation value

$$\Delta_v(z) = \frac{1}{2}\int_0^L \mathrm{d}z'[\hat{S}^\dagger(z',t)\mathcal{V}(z-z')\hat{S}(z',t)],$$

which refers to the vdW induced shift of state $|r\rangle$. This fully describes the slow-light dynamics of signal ($\hat{\Omega}_s$) yet makes Eq. (2) difficult to solve.

In the spirit of a mean-field sense, we now develop an improved version of the SA model [30] to solve Eq. (2) by providing an estimate of the total Rydberg excitations that is consistent with dynamic equations for SAs as well as with dynamic equations for atoms. Each SA is defined here as an ensemble of $n_b = NV_b$ atoms in the thin and short cylinder of volume $V_b = 2\pi R_b R_s^2$ with half blockade length $R_b = [C_6(\delta^2+\gamma_e^2)/(\delta+\gamma_e)|\Omega_c|^2]^{1/6}$ [48] and signal beam radius $R_s \le R_b$. The SAs should be described by 3^{n_b} collective states among which $|G\rangle$ is the ground state while $|E^{(1)}\rangle$ and $|R^{(1)}\rangle$ are the first-order states [31]. Higher-order SA states involving two or more excitations in atomic state $|r\rangle$ ($|e\rangle$) can be safely ignored because they are strictly forbidden (greatly suppressed) owing to the dipole blockade (EIT) effect [31] in the parameter regime of our interest. Then we can define $\hat{\Sigma}_{IJ} = |I\rangle\langle J|$ as the SA transition ($I \neq J$) or projection ($I = J$) operators with $\{I, J\} \in \{G, E^{(1)}, R^{(1)}\}$.

For the n_b atoms in a given SA, their (average) vdW induced shift can be expressed as $\Delta_v = \bar{\Delta}\Sigma_{RR} + \bar{\delta}\bar{\Sigma}_{RR}$, being $\bar{\Delta} \to \infty$ weighted by the local Rydberg population Σ_{RR} inside of this SA while $\bar{\delta} = \Omega_c^2/(8\gamma_e)$ weighted by the average Rydberg population $\bar{\Sigma}_{RR}$ outside of this SA [30, 31]. As shown in the next section, both Σ_{RR} and $\bar{\Sigma}_{RR}$ are very small and of the same order, so it is appropriate to take $\Delta_v = \bar{\Delta}\Sigma_{RR}$ in the following. Accordingly, we have a two-level absorbing system for the Σ_{RR} fraction of SAs after taking $\bar{\Delta} \to \infty$ into Eq. (2), while a three-level EIT system for the $1-\Sigma_{RR}$ fraction of SAs after taking $\bar{\Delta} \to 0$ into Eq. (2) [49]. Then, replacing operators $\hat{O}$ with their expectation values O, we can recast Eq. (2) into the following set of coupled equations

$$\begin{aligned}
\partial_t\Sigma_{GG} &= 2\gamma_e\Sigma_{EE} - \mathrm{i}\sqrt{n_b}\Omega_s\Sigma_{EG} + \mathrm{i}\sqrt{n_b}\Omega_s^*\Sigma_{GE},\\
\partial_t\Sigma_{EE} &= -2\gamma_e\Sigma_{EE} + 2\gamma_r\Sigma_{RR} - \mathrm{i}\Omega_c\Sigma_{RE} + \mathrm{i}\Omega_c^*\Sigma_{ER}\\
&\quad + \mathrm{i}\sqrt{n_b}\Omega_s\Sigma_{EG} - \mathrm{i}\sqrt{n_b}\Omega_s^*\Sigma_{GE},\\
\partial_t\Sigma_{GE} &= -(\gamma_e - \mathrm{i}\delta)\Sigma_{GE} + \mathrm{i}\Omega_c^*\Sigma_{GR}\\
&\quad - \mathrm{i}\sqrt{n_b}\Omega_s(\Sigma_{EE} - \Sigma_{GG}),\\
\partial_t\Sigma_{GR} &= -(\gamma_r - \mathrm{i}\Delta)\Sigma_{GR} + \mathrm{i}\Omega_c\Sigma_{GE} - \mathrm{i}\sqrt{n_b}\Omega_s\Sigma_{ER},\\
\partial_t\Sigma_{ER} &= -(\gamma_e + \gamma_r - \mathrm{i}\Delta + \mathrm{i}\delta)\Sigma_{ER}\\
&\quad - \mathrm{i}\Omega_c(\Sigma_{RR} - \Sigma_{EE}) - \mathrm{i}\sqrt{n_b}\Omega_s^*\Sigma_{GR},
\end{aligned} \tag{3}$$

for the three-level SA;

$$\partial_t P_2 = -(\gamma_e - \mathrm{i}\delta)P_2 + \mathrm{i}\sqrt{N}\Omega_s, \tag{4}$$

for the two-level atom;

$$\begin{aligned}
\partial_t P_3 &= -(\gamma_e - \mathrm{i}\delta)P_3 + \mathrm{i}\Omega_c^* S + \mathrm{i}\sqrt{N}\Omega_s,\\
\partial_t S &= -(\gamma_r - \mathrm{i}\Delta)S + i\Omega_c P_3,
\end{aligned} \tag{5}$$

for the three-level atom;

$$c\partial_z\Omega_s = \mathrm{i}\kappa^2 V\sqrt{N}[P_2\Sigma_{RR} + P_3(1-\Sigma_{RR})], \tag{6}$$

for the signal field. These equations are attained indeed with the following few considerations. First, we work in a regime where the SA population Σ_{RR} is much larger than its atomic counterpart σ_{rr} and non negligible even for very weak signals [50]; all elements Σ_{IJ} have then been included in Eq. (3) with the constraints $\Sigma_{IJ} = \Sigma_{JI}^*$ and $\Sigma_{GG}+\Sigma_{EE}+\Sigma_{RR} = 1$. Second, we remove the term $\partial_t\Omega_s$ from the left side of Eq. (6) as appropriate to the slow-light regime of our interest. Finally, we recall that the two-particle (vdW) interactions will modify the signal's photon statistics, which can be quantified by introducing the two-photon correlation function [31, 51]

$$g_s(z,t) = \frac{\langle\hat{\mathcal{E}}_s^\dagger(z,t)\hat{\mathcal{E}}_s^\dagger(z,t)\hat{\mathcal{E}}_s(z,t)\hat{\mathcal{E}}_s(z,t)\rangle}{\langle\hat{\mathcal{E}}_s^\dagger(z,t)\hat{\mathcal{E}}_s(z,t)\rangle\langle\hat{\mathcal{E}}_s^\dagger(z,t)\hat{\mathcal{E}}_s(z,t)\rangle}$$

as further discussed below. It is worth noting that g_s does not appear to modify Σ_{IJ} and thus Ω_s as it is absent in the dynamic equations of both SAs and atoms. Including g_s in the dynamic equations of only SAs would lead to inconsistent estimates on the total Rydberg excitations obtained with Σ_{RR} and $|S|^2$, respectively. Including g_s in the dynamic equations of both SAs and atoms, though generating consistent estimates on the total Rydberg excitations, is also incorrect because a signal field in the single-photon Fock state ($g_s = 0$) becomes decoupled from the Rydberg-EIT medium. Within the present slow-light regime, g_s can be computed with

$$c\partial_z g_s = -\kappa^2 V\sqrt{N}\mathrm{Im}[\Sigma_{RR}(P_2 - P_3)/\Omega_s]g_s, \tag{7}$$

to account for two-particle (vdW) interactions.

With the help of Eqs. (3)–(6) we can now compute the number of *incident* signal photons $N_s^{in} \equiv N_s(z=0)$ and that of *retrieved* signal photons $N_s^{re} \equiv N_s(z=L)$ outside the Rydberg-EIT medium

$$N_s(z) = \frac{\hbar\varepsilon_0\lambda_s R_s^2}{d_{ge}^2}\int_{-\infty}^{\infty}|\Omega_s(z,t)|^2\mathrm{d}t, \tag{8}$$

with the consideration of $N_s(z)\hbar\omega_s = \pi R_s^2\int_0^\infty I_s(z,t)\mathrm{d}t$ as well as $I_s(z,t) = 2\hbar^2 c\varepsilon_0|\Omega_s(z,t)|^2/d_{ge}^2$. The number

of *stored* signal photons inside the Rydberg-EIT medium, however, should be computed with

$$N_s^{st} = \frac{\hbar\varepsilon_0\lambda_s R_s^2}{d_{ge}^2 v_g}\int_0^L |\Omega_s(z,t_1)|^2 \mathrm{d}z, \tag{9}$$

being v_g the group velocity of a slowly propagating signal and t_1 (slightly smaller than t_{off}) the time when the control field starts to decrease. The number of *distributed* Rydberg excitations, in particular, will be estimated in two consistent ways. The *first* is

$$n_{ryd}^{at} = \pi R_s^2 \int_0^L [1-\Sigma_{RR}(z,t_2)]|S(z,t_2)|^2 \mathrm{d}z, \tag{10}$$

which denotes the total Rydberg excitations contributed by the $(1-\Sigma_{RR})$ fraction of atoms, *i.e.*, those described by the three-level EIT configuration, since $\pi R_s^2|S|^2\mathrm{d}z = N|\sigma_{rr}|\mathrm{d}V$. It is then appropriate to further introduce the effective spin field $S' = S\sqrt{1-\Sigma_{RR}}$ by excluding all two-level absorbing atoms. The *second* is

$$n_{ryd}^{sa} = \frac{1}{2R_b}\int_0^L \Sigma_{RR}(z,t_2)\mathrm{d}z, \tag{11}$$

which denotes the total Rydberg excitations contributed by all $L/2R_b$ *SA*s with $\int_0^L(\Sigma_{RR}/L)dz$ being the average population. Here t_2 (slightly larger than t_{off}) is the time when the control field just decreases to zero.

The steady state solutions of Eq. (5) and Eq. (6)

$$P_2 = \sqrt{N}\sigma_{ge}^{(2)} = \frac{\mathrm{i}\sqrt{N}\Omega_s}{\gamma_e - \mathrm{i}\delta}, \tag{12a}$$

$$P_3 = \sqrt{N}\sigma_{ge}^{(3)} = \frac{i(\gamma_r - \mathrm{i}\Delta)\sqrt{N}\Omega_s}{(\gamma_e-\mathrm{i}\delta)(\gamma_r-\mathrm{i}\Delta)+|\Omega_c|^2}, \tag{12b}$$

$$S = \sqrt{N}\sigma_{gr}^{(3)} = \frac{-\sqrt{N}\Omega_s\Omega_c}{(\gamma_e-\mathrm{i}\delta)(\gamma_r-\mathrm{i}\Delta)+|\Omega_c|^2}. \tag{12c}$$

enable one to attain the atomic population

$$\sigma_{rr} \equiv \sigma_{rg}^{(3)}\sigma_{gr}^{(3)} = \frac{|\Omega_s|^2|\Omega_c|^2}{\gamma_e^2\Delta^2 + (|\Omega_c|^2-\delta\Delta)^2}, \tag{13}$$

whose maxima and half maxima are at

$$\Delta_{max} = \delta \times \frac{|\Omega_c^2|}{\delta^2+\gamma_e^2}; \quad \Delta_{half}^{\pm} = (\delta \pm \gamma_e)\times\frac{|\Omega_c^2|}{\delta^2+\gamma_e^2}$$

in the limit of $\gamma_r \to 0$ for a fixed δ. In fact, we have used Δ_{half}^{+} to define the blockade radius R_b because C_6 is positive. With $\chi_s^{(3)} = (1-\Sigma_{RR})N|d_{ge}|^2\sigma_{ge}^{(3)}/(\hbar\varepsilon_0\Omega_s)$, we can also attain the group velocity at $\Delta = 0$

$$v_g = \frac{\lambda_s}{\pi\partial\chi_s^{(3)}/\partial\Delta} = \frac{\hbar\varepsilon_0\lambda_s|\Omega_c|^2}{\pi N|d_{ge}|^2(1-\Sigma_{RR})}, \tag{14}$$

which will change more or less during the slow-light signal propagation depending on the local value of Σ_{RR}. We finally find $N_s^{st} = n_{ryd}^{at}$ and $n_{ryd}^{at} = n_{ryd}^{sa}$ at $\Delta = 0$ by taking $\Sigma_{RR} = n_b|\Omega_s|^2/(n_b|\Omega_s|^2+|\Omega_c|^2)$ [30] and $n_b = 2\pi N R_b R_s^2$ as well as v_g in Eq. (14) and S in Eq. (12c) back to Eqs. (9)–(11). The former equality $N_s^{st} = n_{ryd}^{at}$ suggests that a Rydberg dark-state polariton [43] is formed as the number of stored signal photons is identical to the number of total Rydberg excitations. The latter equality $n_{ryd}^{at} = n_{ryd}^{sa}$ [52] is naturally required in a valid SA model as both n_{ryd}^{at} and n_{ryd}^{sa} refer to the number of total Rydberg excitations, though attained from dynamic equations of atoms and those of SAs, respectively.

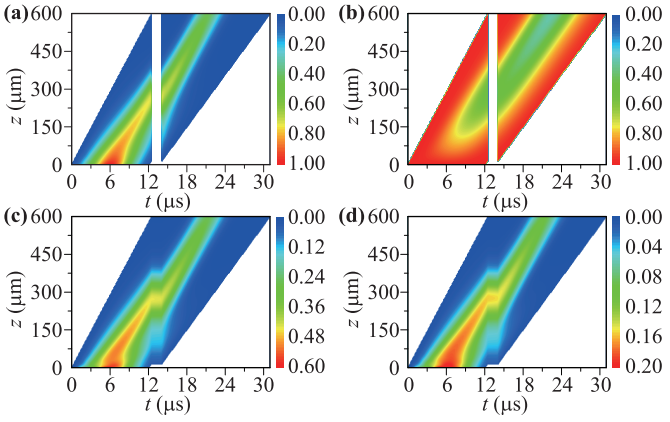

Fig. 2 Space-time evolutions of the scaled pulse intensity $|\Omega_s/\Omega_s^m|^2$ **(a)**, the two-photon correlation g_s **(b)**, the scaled magnitude square of spin field $10^5|S'|^2/N$ **(c)**, and the SA Rydberg population Σ_{RR} **(d)** in case (i). The control and signal fields have parameters $\Delta = 0$, $\Omega_c = 2\pi\times 2.3$ MHz, $\delta = 2\pi\times 18$ MHz, $\Omega_s^m = 2\pi\times 6.0$ kHz, $t_s = 6.0$ μs, $\delta t_s = 5.0$ μs, $t_{off} = 12.5$ μs, $t_{on} = 14.0$ μs, $\lambda_s = 780$ nm, and $R_s = 14.0$ μm. The Rydberg-EIT medium has parameters $\gamma_e = 2\pi\times 6.0$ MHz, $\gamma_r = 2\pi\times 2.0$ kHz, $d_{ge} = 2.534\times 10^{-29}$ C·m, $N_0 = 1.8\times 10^{12}$ cm^{-3}, $L = 600$ μm, and $R_b = 16.4$ μm.

3 Results and discussion

In this section, we present numerical simulations on the nontrivial slow-light propagation in a cold Rydberg-EIT medium under two-photon resonance ($\Delta = 0$) using the improved SA model. In particular, we aim at examining whether storing the same number of signal photons can be realized with different combinations of δ and Ω_s^m and in the presence of different dynamic behaviors. The simulations proceed from an incident (Gaussian) signal with field amplitude $\Omega_s(0,t) = \Omega_s^m \mathrm{e}^{-(t-t_s)^2/\delta t_s^2}$ and two-photon correlation $g_s(0,t) = 1$, as appropriate for an ideal (coherent state) laser. These numerical results enable us to ascertain two representative cases of the pulse dynamics: (i) the incident signal is a well detuned weaker pulse with $\Omega_s^m/(2\pi) = 6$ kHz ($N_s^{in} \simeq 2.0$) and $\delta/(2\pi) = 18$ MHz, and (ii) the incident signal is a nearly resonant stronger pulse with $\Omega_s^m/(2\pi) = 16$ kHz ($N_s^{in} \simeq 14.0$) and $\delta/(2\pi) = 8$ MHz. The two cases confirm that storing the $N_s^{st} \simeq 1.0$

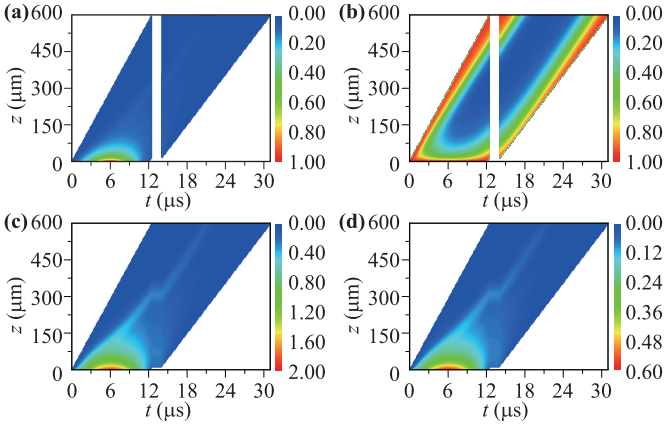

Fig. 3 Space-time evolutions of the scaled pulse intensity $|\Omega_s/\Omega_s^m|^2$ **(a)**, the two-photon correlation g_s **(b)**, the scaled magnitude square of spin field $10^5|S'|^2/N$ **(c)**, and the SA Rydberg population Σ_{RR} **(d)** in case (ii). Parameters used in simulations are the same as in Fig. 2 except $\Omega_s^m = 2\pi\times 16$ kHz, $\delta = 2\pi\times 8$ MHz, and $R_b = 14.2$ μm.

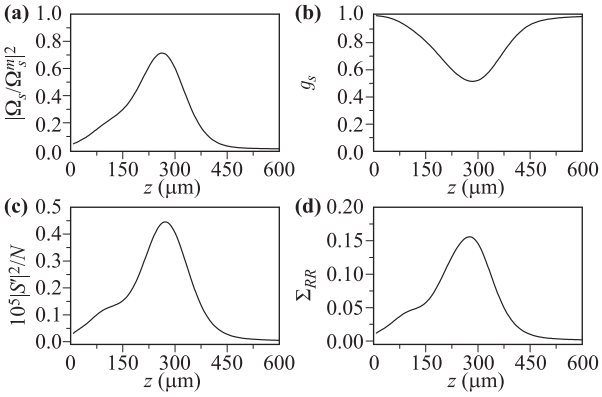

Fig. 4 Spatial profiles of the scaled pulse intensity $|\Omega_s/\Omega_s^m|^2$ **(a)**, the two-photon correlation g_s **(b)**, the scaled magnitude square of spin field $10^5|S'|^2/N$ **(c)**, and the SA Rydberg population Σ_{RR} **(d)** with the same set of parameters as in Fig. 2 [case (i)] except $t_1 = 12.4$ μs for $|\Omega_s/\Omega_s^m|^2$ and g_s while $t_2 = 12.6$ μs for $10^5|S'|^2/N$ and Σ_{RR}.

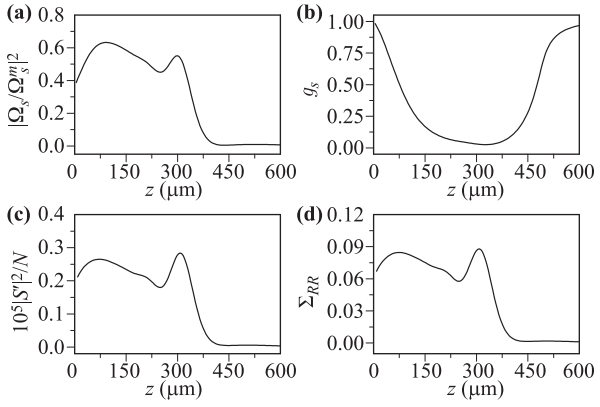

Fig. 5 Spatial profiles of the scaled pulse intensity $|\Omega_s/\Omega_s^m|^2$ **(a)**, the two-photon correlation g_s **(b)**, the scaled magnitude square of spin field $10^5|S'|^2/N$ **(c)**, and the SA Rydberg population Σ_{RR} **(d)** with the same set of parameters as in Fig. 3 [case (ii)] except $t_1 = 12.4$ μs for $|\Omega_s/\Omega_s^m|^2$ and g_s while $t_2 = 12.6$ μs for $10^5|S'|^2/N$ and Σ_{RR}.

signal photon may be achieved with different storage and retrieval efficiencies and different two-photon correlation reductions owing to different dynamic behaviors.

Figure 2 shows for case (i) four characteristic space-time propagation variables, namely, the two-photon correlation (g_s), the spin field ($|S'|^2$), the SA Rydberg population (Σ_{RR}), and the pulse intensity ($|\Omega_s|^2$). The signal is seen to move at a group velocity $v_g \simeq 43.2$ m/s in that it travels through the medium of 600 μm length during the 13.89 μs interval (after subtracting the 1.5 μs storage time), which is also consistent with an estimation based on Eq. (14). These variables are increasingly attenuated during the slow-light signal propagation depending on the local values of Σ_{RR} and $|\Omega_s|^2$. It can be understood from Eqs. (3)–(6) that a larger $|\Omega_s|^2$ results in a higher Rydberg excitation characterized by Σ_{RR} and $|S'|^2$ while a larger Σ_{RR} results in a stronger attenuation of $|\Omega_s|^2$ and g_s. As the control field is turned off (on), the slowly propagating $|\Omega_s|^2$ and g_s are mapped into (recovered from) the stationary Σ_{RR} and $|S'|^2$, which stop decreasing when $|\Omega_s|^2 = 0$ leads to $P_2 = P_3 = 0$. It is also clear that $|S'|^2$ and Σ_{RR} have almost identical space-time profiles during the slow-light signal propagation as they both describe the distributed Rydberg excitations.

Figure 3 shows that in case (ii) similar slow-light ($v_g \simeq 42.8$ m/s) dynamics occurs for $|\Omega_s|^2$ and g_s as well as $|S'|^2$ and Σ_{RR}. Compared to case (i), the main difference lies in that these variables suffer a stronger/quicker attenuation during dynamic propagation because a larger signal field intensity $|\Omega_s|^2$ yields a higher SA Rydberg population Σ_{RR}. Note, in particular, that we have $\Sigma_{RR} \simeq 0.6$ close to the entrance $z = 0$ when $|\Omega_s|^2$ is not severely attenuated yet. This indicates that a clear difference can be found between the space-time profiles of $|S|^2$ and Σ_{RR} (not shown here) at the early stage of slow-light propagation, though $|S'|^2$ and Σ_{RR} are almost identical. Note also that a weaker/slower attenuation of these variables has been observed for very small Σ_{RR} close to the exit $z = L$ where the linear absorption arising from $\mathtt{Im}P_3$ is dominant because the nonlinear absorption arising from $\mathtt{Im}P_2$ is evident only for large Σ_{RR}.

Figure 4 shows typical spatial profiles for $|\Omega_s|^2$ and g_s as Ω_c starts to decrease while for $|S'|^2$ and Σ_{RR} as Ω_c decreases to zero in case (i), from which it is easy to attain $n_{ryd}^{at} \simeq n_{ryd}^{sa} \simeq N_s^{st} = 0.997$. This confirms, on one hand, that the two ways based on dynamic equations of SAs or atoms to estimate the number of total Rydberg excitations are consistent while, on the other hand, stored signal photons manifest themselves as spatially distributed Rydberg excitations. Then $\eta_s^{st} = N_s^{st}/N_s^{in} \simeq 50.6\%$ is the storage efficiency of this single-photon-level signal field,

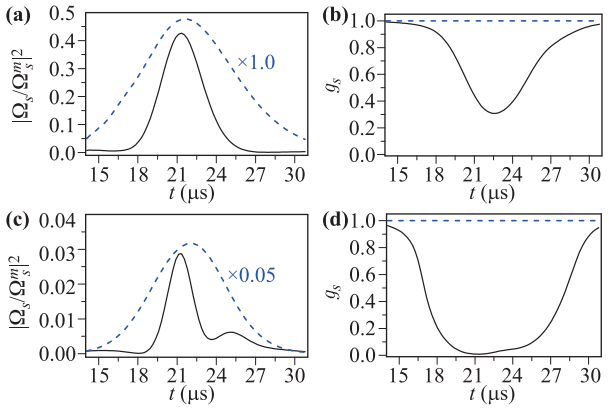

Fig. 6 Temporal profiles of the scaled pulse intensity $|\Omega_s/\Omega_s^m|^2$ **(a, c)** and the two-photon correlation g_s **(b, d)**. Parameters are the same as in Fig. 2 [case (i)] for panels **(a, b)** while as in Fig. 3 [case (ii)] for panels **(c, d)** except $z = L$. Blue-dashed curves are attained with $\Sigma_{RR} \equiv 0$ as a reference.

which depends severely on the vdW interactions of Rydberg excitations at different positions. That means, we cannot ignore the vdW interactions even in the case of a single photon as it will lead to a dark-state polariton with distributed Rydberg excitations.

Figure 5 shows very different spatial profiles as compared to Fig. 4 for the four optical and atomic variables in case (ii) where the incident signal field contains more photons yet at a smaller detuning. We find that $|\Omega_s|^2$ and g_s suffer a severer attenuation in the presence of a stronger nonlinear absorption contributed by $\mathtt{Im}P_2$, and further notice that $|\Omega_s|^2$, $|S'|^2$, and Σ_{RR} exhibit similar distorted profiles with the leading (trailing) edges being more (less) attenuated after a longer (shorter) traveling journey. Our calculated figures $n_{ryd}^{at} \simeq n_{ryd}^{sa} \simeq N_s^{st} = 0.936$, together with the roughly identical but clearly asymmetric profiles of $|\Omega_s|^2$, $|S'|^2$, and Σ_{RR}, confirm again that the two ways used to estimate the number of total Rydberg excitations are consistent; a single-photon-level signal field can be stored into distributed Rydberg excitations, though at a lower efficiency $\eta_s^{st} = N_s^{st}/N_s^{in} \simeq 6.6\%$.

Figure 6 shows that the retrieved signal field is more symmetric with a less distorted profile than the stored signal field in both cases (i) and (ii). The underlying physics could be attributed to that, during the retrieval process, the trailing edge suffers more nonlinear absorption than the leading edge because it is stronger and travels a longer journey. But it is impractical to eliminate the profile distortion, which is more evident in case (ii) manifesting as a clear splitting [53], owing to the inevitable nonlinear dispersion in both storage and retrieval processes. With the retrieved signal profiles, we can calculate the number of retrieved photons, which turns out to be $N_s^{re} \simeq 0.539$ with a higher efficiency $\eta_s^{re} = N_s^{re}/N_s^{in} \simeq 27.3\%$ in case (i) while $N_s^{re} \simeq 0.211$ with a lower efficiency $\eta_s^{re} = N_s^{re}/N_s^{in} \simeq$ 1.5% in case (ii). These figures of N_s^{re} are clearly smaller than their counterparts of N_s^{st} (see Table 1) because the retrieved signal field suffers extra nonlinear absorption in its trailing edge. Blue-dashed curves are calculated for a normal EIT medium to show that little differences can be found between cases (i) and (ii) in the presence of only linear absorption and dispersion.

Table 1 Signal photon numbers, total Rydberg excitations, and storage/retrieval efficiencies in two specific cases.

Case	N_s^{in}	N_s^{st} (η_s^{st})	n_{ryd}^{at}	n_{ryd}^{sa}	N_s^{re} (η_s^{re})
(i)	1.97	0.997 (50.6%)	0.994	0.995	0.539 (27.3%)
(ii)	14.1	0.936 (6.6%)	0.930	0.939	0.211 (1.5%)

Finally, comparing the above numerical results suggests that the attenuation and distortion of a retrieved signal field are likely to be suppressed by choosing the combination of a larger δ and a smaller Ω_s^m. In other words, a higher retrieval efficiency and a well preserved profile apply only to a well detuned weaker signal field as considered in case (i) because this choice is helpful to greatly reduce the nonlinear absorption and dispersion. Nevertheless, it is also meaningful to choose the combination of a smaller δ and a larger Ω_s^m as considered in case (ii) because this choice is beneficial to generate quasi-deterministic single photons [21] characterized by $g_s \to 0$. In fact, one main difference between a Rydberg-EIT medium and a normal EIT medium lies in that the former allows to modify photonic statistics of a signal field during its slow-light propagation. We further find it instructive to account for the attenuation and distortion of a signal field via its state fidelity by calculating the overlap of outgoing and incoming spectra [54], which is equivalent indeed to the temporal integral $\sqrt{F_s} = |\int \Omega_s(0,t)\Omega_s(L,t)\mathrm{d}t|/\int |\Omega_s(0,t)|^2\mathrm{d}t$ as warranted by the Parseval's theorem. It is then straightforward to attain $F_s \simeq 0.566$ in case (i) while $F_s \simeq 0.124$ in case (ii) by taking $\Omega_s(0,t)$ and $\Omega_s(L,t)$ as the incoming and outgoing signals, respectively.

4 Conclusion

In summary, we have studied the slow-light dynamics of a few-photons signal pulse traveling through a cold Rydberg-EIT medium via an improved SA model, which provide a consistent treatment on the number of total Rydberg excitations. Numerical calculations show in particular that it is viable to achieve light storage and retrieval with higher (lower) efficiencies and well preserved (more distorted) profiles when a weaker (stronger) signal pulse is incident at a larger (smaller) detuning. The underlying physics can be attributed to spatially distributed Rydberg excitations, depending critically on the local intensity of signal pulses as a result of nonlocal vdW interactions. Our results are believed to contribute a new insight onto yet unclear aspects of experiments with respect to

single-photon-level light storage in cold Rydberg atoms, and be relevant for further works on photonic information processing with cold Rydberg atoms.

Acknowledgements The work was supported by the National Natural Science Foundation of China (Nos. 11534002 and 12074061), and the Cooperative Program by the Italian Ministry of Foreign Affairs and International Cooperation (No. PGR00960), and the National Natural Science Foundation of China (No. 11861131001).

References and notes

1. A. K. Ekert, Quantum cryptography based on Bell's theorem, *Phys. Rev. Lett.* 67(6), 661 (1991)
2. H. P. Zeng, G. Wu, E. Wu, H. F. Pan, C. Y. Zhou, F. Treussart, and J. F. Roch, Generation and detection of infrared single photons and their applications, *Front. Phys. China* 1(1), 1 (2006)
3. L. M. Duan, M. D. Lukin, J. I. Cirac, and P. Zoller, Long distance quantum communication with atomic ensembles and linear optics, *Nature* 414(6862), 413 (2001)
4. E. Knill, R. Laflamme, and G. J. Milburn, A scheme for efficient quantum computation with linear optics, *Nature* 409(6816), 46 (2001)
5. K. M. Birnbaum, A. Boca, R. Miller, A. D. Boozer, T. E. Northup, and H. J. Kimble, Photon blockade in an optical cavity with one trapped atom, *Nature* 436(7047), 87 (2005)
6. Y. Colombe, T. Steinmetz, G. Dubois, F. Linke, D. Hunger, and J. Reichel, Strong atom-field coupling for Bose–Einstein condensates in an optical cavity on a chip, *Nature* 450(7167), 272 (2007)
7. A. Kubanek, A. Ourjoumtsev, I. Schuster, M. Koch, P. W. H. Pinkse, K. Murr, and G. Rempe, Two-photon gateway in one-atom cavity quantum electrodynamics, *Phys. Rev. Lett.* 101(20), 203602 (2008)
8. M. Fleischhauer, A. Imamoglu, and J. P. Marangos, Electromagnetically induced transparency: Optics in coherent media, *Rev. Mod. Phys.* 77(2), 633 (2005)
9. C. Möhl, N. L. R. Spong, Y. C. Jiao, C. So, T. Ilieva, M. Weidemüller, and C. S. Adams, Photon correlation transients in a weakly blockaded Rydberg ensemble, *J. Phys. At. Mol. Opt. Phys.* 53(8), 084005 (2020)
10. Z. Y. Shen, H. L. Yang, X. Liu, X. J. Huang, T. Y. Xiang, J. Wu, and W. Chen, Electromagnetically induced transparency in novel dual-band metamaterial excited by toroidal dipolar response, *Front. Phys.* 15(1), 12601 (2020)
11. C. Ottaviani, D. Vitali, M. Artoni, F. Cataliotti, and P. Tombesi, Polarization qubit phase gate in driven atomic media, *Phys. Rev. Lett.* 90(19), 197902 (2003)
12. Z. B. Wang, K. P. Marzlin, and B. C. Sanders, Large cross-phase modulation between slow copropagating weak pulses in ^{87}Rb, *Phys. Rev. Lett.* 97(6), 063901 (2006)
13. B. W. Shiau, M. C. Wu, C. C. Lin, and Y. C. Chen, Lowlight-level cross-phase modulation with double slow light pulses, *Phys. Rev. Lett.* 106(19), 193006 (2011)
14. M. Saffman, T. G. Walker, and K. Molmer, Quantum information with Rydberg atoms, *Rev. Mod. Phys.* 82(3), 2313 (2010)
15. J. Hwang, M. Pototschnig, R. Lettow, G. Zumofen, A. Renn, S. Götzinger, and V. Sandoghdar, A single-molecule optical transistor, *Nature* 460(7251), 76 (2009)
16. J. D. Pritchard, K. J. Weatherill, and C. S. Adams, Nonlinear optics using cold Rydberg atoms, *Annu. Rev. Cold At. Mol.* 1, 301 (2013)
17. O. Firstenberg, C. S. Adams, and S. Hofferberth, Nonlinear quantum optics mediated by Rydberg interactions, *J. Phys. At. Mol. Opt. Phys.* 49(15), 152003 (2016)
18. Y. O. Dudin and A. Kuzmich, Strongly interacting Rydberg excitations of a cold atomic gas, *Science* 336(6083), 887 (2012)
19. H. Gorniaczyk, C. Tresp, J. Schmidt, H. Fedder, and S. Hofferberth, Single-photon transistor mediated by interstate Rydberg interactions, *Phys. Rev. Lett.* 113(5), 053601 (2014)
20. D. Tiarks, S. Schmidt, G. Rempe, and S. Durr, Optical π phase shift created with a single-photon pulse, *Sci. Adv.* 2(4), e1600036 (2016)
21. A. Padrón-Brito, R. Tricarico, P. Farrera, E. Distante, K. Theophilo, D. Chang, and H. de Riedmatten, Transient dynamics of the quantum light retrieved from Rydberg polaritons, *New J. Phys.* 23(6), 063009 (2021)
22. J. D. Pritchard, D. Maxwell, A. Gauguet, K. J. Weatherill, M. P. A. Jones, and C. S. Adams, Cooperative atom–light interaction in a blockade Rydberg ensemble, *Phys. Rev. Lett.* 105(19), 193603 (2010)
23. P. Bienias, S. Choi, O. Firstenberg, M. F. Maghrebi, M. Gullans, M. D. Lukin, A. V. Gorshkov, and H. P. Buchler, Scattering resonances and bound states for strongly interacting Rydberg polaritons, *Phys. Rev. A* 90(5), 053804 (2014)
24. M. F. Maghrebi, M. J. Gullans, P. Bienias, S. Choi, I. Martin, O. Firstenberg, M. D. Lukin, H. P. Buchler, and A. V. Gorshkov, Coulomb bound states of strongly interacing photons, *Phys. Rev. Lett.* 115(12), 123601 (2015)
25. M. Moos, R. Unanyan, and M. Fleischhauer, Creation and detection of photonic molecules in Rydberg gases, *Phys. Rev. A* 96(2), 023853 (2017)
26. M. D. Lukin, M. Fleischhauer, R. Côté, L. M. Duan, D. Jaksch, J. I. Cirac, and P. Zoller, Dipole blockade and quantum information processing in mesoscopic atomic ensembles, *Phys. Rev. Lett.* 87(3), 037901 (2001)
27. D. Tong, S. M. Farooqi, J. Stanojevic, S. Krishnan, Y. P. Zhang, R. Côté, E. E. Eyler, and P. L. Gould, Local blockade of Rydberg excitation in an ultracold gas, *Phys. Rev. Lett.* 93(6), 063001 (2004)
28. K. Singer, M. Reetz-Lamour, T. Amthor, L. G. Marcassa, and M. Weidemuller, Suppression of excitation and spectral broadening induced by interactions in a cold gas of Rydberg atoms, *Phys. Rev. Lett.* 93(16), 163001 (2004)
29. X. F. Shi, Rydberg quantum computation with nuclear spins in two-electron neutral atoms, *Front. Phys.* 16(5), 52501 (2021)

30. D. Petrosyan, J. Otterbach, and M. Fleischhauer, Electromagnetically induced transparency with Rydberg atoms, *Phys. Rev. Lett.* 107(21), 213601 (2011)
31. Y. M. Liu, D. Yan, X. D. Tian, C. L. Cui, and J. H. Wu, Electromagnetically induced transparency with cold Rydberg atoms: Superatom model beyond the weak-probe approximation, *Phys. Rev. A* 89(3), 033839 (2014)
32. X. D. Tian, Y. M. Liu, Q. Q. Bao, J. H. Wu, M. Artoni, and G. C. La Rocca, Nonclassical storage and retrieval of a multi-photon pulse in cold Rydberg atoms, *Phys. Rev. A* 97(4), 043811 (2018)
33. D. Maxwell, D. J. Szwer, D. Paredes-Barato, H. Busche, J. D. Pritchard, A. Gauguet, K. J. Weatherill, M. P. A. Jones, and C. S. Adams, Storage and control of optical photons using Rydberg polaritons, *Phys. Rev. Lett.* 110(10), 103001 (2013)
34. C. S. Hofmann, G. Günter, H. Schempp, M. Robert-de-Saint-Vincent, M. Gärttner, J. Evers, S. Whitlock, and M. Weidemüller, Sub-Poissonian statistics of Rydberg interacting dark-state polaritons, *Phys. Rev. Lett.* 110(20), 203601 (2013)
35. E. Distante, A. Padron-Brito, M. Cristiani, D. Paredes-Barato, and H. de Riedmatten, Storage enhanced nonlinearities in a cold atomic Rydberg ensemble, *Phys. Rev. Lett.* 117(11), 113001 (2016)
36. F. Ripka, Y. H. Chen, R. Low, and T. Pfau, Rydberg polaritons in a thermal vapor, *Phys. Rev. A* 93(5), 053429 (2016)
37. L. Li and A. Kuzmich, Quantum memory with strong and contollable Rydberg-level interactions, *Nat. Commun.* 7(1), 13618 (2016)
38. E. Distante, P. Farrera, A. Padron-Brito, D. Paredes-Barato, G. Heinze, and H. de Riedmatten, Storing single photons emitted by a quantum memory on a highly excited Rydberg state, *Nat. Commun.* 8(1), 14072 (2017)
39. C. S. Hofmann, G. Günter, H. Schempp, N. L. M. Müller, A. Faber, H. Busche, M. Robert-de-Saint-Vincent, S. Whitlock, and M. Weidemüller, An experimental approach for investigating many-body phenomena in Rydberg interacting quantum systems, *Front. Phys.* 9(5), 571 (2014)
40. A. V. Gorshkov, J. Otterbach, M. Fleischhauer, T. Pohl, and M. D. Lukin, Photon–photon interactions via Rydberg blockade, *Phys. Rev. Lett.* 107(13), 133602 (2011)
41. B. He, A. V. Sharypov, J. T. Sheng, C. Simon, and M. Xiao, Two-photon dynamics in coherent Rydberg atomic ensemble, *Phys. Rev. Lett.* 112(13), 133606 (2014)
42. T. Caneva, M. T. Manzoni, T. Shi, J. S. Douglas, J. I. Cirac, and D. E. Chang, Quantum dynamics of propagating photons with strong interactions: A generalized input-output formalism, *New J. Phys.* 17(11), 113001 (2015)
43. M. J. Gullans, J. D. Thompson, Y. Wang, Q. Y. Liang, V. Vuletic, M. D. Lukin, and A. V. Gorshkov, Effective field theory for Rydberg polaritons, *Phys. Rev. Lett.* 117(11), 113601 (2016)
44. W. B. Li, D. Viscor, S. Hofferberth, and I. Lesanovsky, Electromagnetically induced transparency in an entangled medium, *Phys. Rev. Lett.* 112(24), 243601 (2014)
45. R. Loudon, The Quantum Theory of Light, 3rd Ed., Oxford Science Publications, 2000
46. Here and in what follows we choose O as the expectation value of operator $\hat{O}$ by removing its hat.
47. L. Yang, B. He, J. H. Wu, Z. Y. Zhang, and M. Xiao, Interacting photon pulses in a Rydberg medium, *Optica* 3(10), 1095 (2016)
48. This quantity is usually called blockade radius and will reduce to $R_b = (C_6\gamma_e/|\Omega_c|^2)^{1/6}$ in the case of $\delta = 0$ while to $R_b = (C_6\delta/|\Omega_c|^2)^{1/6}$ inthe case of $\delta \gg \gamma_e$.
49. This conclusion holds also for the attractive vdW interactions denoted by a negative C_6 and thus $\bar{\Delta} \to -\infty$ (instead of $\bar{\Delta} \to \infty$) for the Σ_{RR} fraction of SAs.
50. In fact, we can make n_b sufficiently large to yield a remarkably enhanced collective coupling ($\sqrt{n_b}\Omega_s$).
51. O. Firstenberg, T. Peyronel, Q. Y. Liang, A. V. Gorshkov, M. D. Lukin, and V. Vuletić, Attractive photons in a quantum nonlinear medium, *Nature* 502(7469), 71 (2013)
52. This equality is equivalent after proper arrangement to Eq. (10) in [M. Garttner, S. Whitlock, D. W. Schonleber, and J. Evers, *Phys. Rev. A* 89(06), 063407 (2014)].
53. C. Shou and G. X. Huang, Slow-light soliton beam splitters, *Phys. Rev. A* 99(4), 043821 (2019)
54. J. Gea-Banacloche and N. Nemet, Conditional phase gate using an optomechanical resonator, *Phys. Rev. A* 89(5), 052327 (2014)